Disk surface density transitions as protoplanet traps

F. S. Masset[1,2]

SAp, Orme des Merisiers, CE-Saclay, 91191 Gif/Yvette Cedex, France

fmasset@cea.fr

A. Morbidelli, A. Crida

Laboratoire Cassiopée - CNRS/UMR 6202, Observatoire de la Côte d'Azur, BP 4229, 06304 Nice Cedex 4, France

morby@obs-nice.fr, crida@obs-nice.fr

and

J. Ferreira

Laboratoire d'Astrophysique de Grenoble, 414 rue de la piscine, BP 53, 38041 Grenoble Cedex 9, France

Jonathan.Ferreira@obs.ujf-grenoble.fr

ABSTRACT

The tidal torque exerted by a protoplanetary disk with power law surface density and temperature profiles onto an embedded protoplanetary embryo is generally a negative quantity that leads to the embryo inwards migration. Here we investigate how the tidal torque balance is affected at a disk surface density radial jump. The jump has two consequences :

- it affects the differential Lindblad torque. In particular if the disk is merely empty on the inner side, the differential Lindblad torque almost amounts to the large negative outer Lindblad torque.
- It affects the corotation torque, which is a quantity very sensitive to the local gradient of the disk surface density. In particular if the disk is depleted on the inside and if the jump occurs radially over a few pressure scale-heights, the corotation torque is a positive quantity that is much larger than in a power-law disk.

[1]Also at IA-UNAM, Ciudad Universitaria, Apartado Postal 70-264, Mexico DF 04510, Mexico

[2]Send offprint requests to fmasset@cea.fr

We show by means of customized numerical simulations of low mass planets embedded in protoplanetary nebulae with a surface density jump that the second effect is dominant, that is that the corotation torque largely dominates the differential Lindblad torque on the edge of a central depletion, even a shallow one. Namely, a disk surface density jump of about 50 % over $3-5$ disk thicknesses suffices to cancel out the total torque. As a consequence the type I migration of low mass objects reaching the jump should be halted, and all these objects should be trapped there provided some amount of dissipation is present in the disk to prevent the corotation torque saturation. As dissipation is provided by turbulence, which induces a jitter of the planet semi-major axis, we investigate under which conditions the trapping process overcomes the trend of turbulence to induce stochastic migration across the disk. We show that a cavity with a large outer to inner surface density ratio efficiently traps embryos from 1 to 15 $M_\oplus$, at any radius up to 5 AU from the central object, in a disk which has same surface density profile as the Minimum Mass Solar Nebula (MMSN). Shallow surface density transitions require light disks to efficiently trap embryos. In the case of the MMSN, this could happen in the very central parts ($r < 0.03$ AU). We discuss where in a protoplanetary disk one can expect a surface density jump. This effect could constitute a solution to the well known problem that the build up of the first protogiant solid core in a disk takes much longer than its type I migration towards the central object.

Subject headings: Planetary systems: formation — planetary systems: protoplanetary disks — Accretion, accretion disks — Methods: numerical — Hydrodynamics

1. Introduction

The migration of low mass protoplanets ($M_p < 15\ M_\oplus$) under the action of disk tides is long known to be a fast process in disks with power law surface density profiles (Ward 1997; Tanaka et al. 2002). The fast migration timescale estimates of these objects even constitutes a bottleneck for the core accretion scenario, which implies a slow build up of a solid core until it reaches the mass threshold ($\sim 15\ M_\oplus$) above which rapid gas accretion begins. Indeed, the solid core build up time is 10^{6-7} yrs (Pollack et al. 1996), while the migration timescale of a $M_p = 1\ M_\oplus$ planet is $O(10^5)$ yrs (Ward 1997; Tanaka et al. 2002) and scales inversely proportionally to the planet mass. The existence of gaseous giant planets at large distances ($a \sim 0.1 - 10$ AU) from their central star therefore constitutes a puzzle. Recent work by

Alibert et al. (2005) has shown that the core build up time scale can be lowered by taking migration into account, which prevents the depletion of the core feeding zone. However, these authors find that the most up to date type I migration timescale estimate, which includes three dimensional effects and the co-rotation torque (Tanaka et al. 2002), still needs to be lowered by a factor $10 - 100$ in order to allow for the solid core survival. The total torque exerted by the disk onto the planet can be split into two parts: the differential Lindblad torque, that corresponds to the torque of the spiral wake that the planet excites in the disk, and the corotation torque, exerted by the material located in the planet coorbital region. The role of the corotation torque has often been overlooked in migration rate estimates. The two main reasons for that is that it is harder to evaluate than the differential Lindblad torque, and that it saturates (i.e. tends to zero) in the absence of dissipation. The corotation torque scales with the radial gradient of Σ/B, where Σ is the disk surface density and B is the second Oort's constant, or half the disk flow vorticity vertical component in a non-rotating frame. This scaling makes the corotation torque a quantity very sensitive to local variations of the disk surface density or rotation profile. Here we investigate the behavior of the total (Lindblad + corotation) tidal torque exerted on a planet in the vicinity of a surface density radial jump, in order to investigate a suggestion by Masset (2002) that localized, positive surface density jumps may be able to halt migration. We assume that the surface density transition occurs on a length scale λ of a few pressure scale heights H. We consider the case in which the surface density is larger on the outside of the transition, but we do not limit ourselves to the case where the surface density on the inside is negligible compared to its value on the outer side. The case of a virtually empty central cavity has already been contemplated by Kuchner & Lecar (2002) in the context, different of ours, of giant planet migration. They conclude that giant planet migration is halted or considerably slowed down once the planet is inside the cavity and in $2:1$ resonance with the cavity edge, as beyond this resonance the disk torque onto a planet on a circular orbit becomes negligible.

In section 2 we provide simple analytical estimates of the Lindblad and corotation torques at a surface density transition. We show that the corotation torque, which is a positive quantity there, is likely to overcome the Lindblad torque if the transition is localized enough, i.e. $\lambda <$ a few H. In section 3 we describe the numerical setup that we used to check this prediction with a numerical hydro-code. In section 4, we present the results of our numerical simulations which indeed exhibit for a wide range of parameters a fixed point at the transition, i.e. a point where the corotation and Lindblad torques cancel each other and where planetary migration stops. We also discuss in this section the issue of the saturation of the corotation torque and the need of turbulence to prevent it, and the conditions under which turbulence is able or not to unlock a planet from the transition. We then discuss in section 5 where in protoplanetary disks such surface density transitions can be found, and

what are the consequences of these planet traps on giant planet formation.

2. A simple analytic estimate

A protoplanet embedded in a gaseous protoplanetary disk excites in the latter a one-armed spiral wake (Ogilvie & Lubow 2002), as a result of the constructive interference of propagative density waves excited at Lindblad resonances with the planet. This wake exerts a torque on the planet, which can be decomposed into the outer Lindblad torque (Γ_o), which is negative and that is exerted by the outer arm, and the inner Lindblad torque (Γ_i), which is positive and that is exerted by the inner arm. These two torques do not cancel out. The residue $\Delta\Gamma = \Gamma_o + \Gamma_i$, called the differential Lindblad torque, is negative (Ward 1986), thereby leading to inward migration. If one calls one-sided Lindblad torque the arithmetic mean of the absolute values of the outer and inner Lindblad torques:

$$\Gamma_{LR} = \frac{\Gamma_i - \Gamma_o}{2}, \tag{1}$$

then the differential Lindblad torque is a fraction of this torque which scales with the disk aspect ratio $h = H/r$, where H is the pressure scale height or disk thickness and r the radius. In particular, for a disk with uniform surface density and aspect ratio (Ward 1997):

$$\Delta\Gamma \approx -8h\Gamma_{LR}. \tag{2}$$

As noted by Ward (1997), in a nebula with $h = O(10^{-1})$, the differential Lindblad torque is a sizable fraction of the one-sided Lindblad torque. This is of some importance for our concern: denoting $\Delta\Gamma'$ the Lindblad torque on an empty cavity edge (it then amounts to the outer Lindblad torque, i.e. $\Delta\Gamma' = \Gamma_o$) and $\Delta\Gamma$ the Lindblad torque further out in the disk where we assume the surface density and aspect ratio profiles to be flat, we have:

$$\Delta\Gamma' \approx \Delta\Gamma/(8h), \tag{3}$$

which means that the Lindblad torque on a cavity edge is at most $2-3$ times larger than further out in the disk, for $0.04 < h < 0.06$.

In addition to the wake torque, the material in the orbit vicinity exerts on the planet the so-called corotation torque. This torque scales with the gradient of the specific vorticity (or vortensity) (Goldreich & Tremaine 1979; Ward 1991, 1992):

$$\Gamma_C \propto \Sigma \cdot \frac{d\log(\Sigma/B)}{d\log r}. \tag{4}$$

This torque comes from the exchange of angular momentum between the planet and fluid elements that perform U-turns at the end of their horseshoe streamlines (Ward 1991; Masset 2001, 2002). It has been estimated that the co-rotation torque amounts to a few tens of percent (Korycansky & Pollack 1993) of the differential Lindblad torque for a disk with a power-law surface density profile. Tanaka et al. (2002) give the following estimate for a three dimensional disk with flat surface density and temperature profiles:

$$\Gamma_C \approx -(1/2)\Delta\Gamma \tag{5}$$

Note that the corotation torque cancels out for a surface density profile $\Sigma \propto r^{-3/2}$, while it is a positive quantity for a shallower surface density profile.

We now estimate the ratio of the corotation torque at a cavity edge and further out in the disk (assuming a flat surface density profile). We assume that the surface density inside of the transition is Σ_i, while it is $\Sigma_o > \Sigma_i$ on the outside. The transition from Σ_i to Σ_o occurs on a length scale $\lambda \ll r$. In the outer disk where $\Sigma \equiv \Sigma_o$, we have:

$$\frac{d\log(\Sigma/B)}{d\log r} = 3/2, \tag{6}$$

while at the transition, $d\log\Sigma/d\log r$ is a sharply peaked function with a maximum that scales as:

$$\left.\frac{d\log\Sigma}{d\log r}\right|_{\max} \sim \frac{r}{\lambda}\log\left(\frac{\Sigma_o}{\Sigma_i}\right). \tag{7}$$

Similarly, retaining only the terms that vary most rapidly with r at the transition:

$$\frac{d\log B}{d\log r} \simeq \frac{2r^2}{\Omega}\frac{d^2\Omega}{dr^2}, \tag{8}$$

where Ω is the angular velocity. The last factor of the above equation can also be expressed, using the disk rotational equilibrium and again keeping only the terms that vary most rapidly with r, as:

$$\frac{d^2\Omega}{dr^2} \simeq -\frac{\Omega h^2 r}{2}\frac{d^3\log\Sigma}{dr^3}. \tag{9}$$

The last factor of the R.H.S. is a function of r that scales as $(H^2 r/\lambda^3)\log(\Sigma_o/\Sigma_i)$, and that has, for a sufficiently smooth, monotonic transition from Σ_i to Σ_o, two minima and one maximum, the exact locations and amplitudes of which depend on the surface density profile. The (inverse of) the specific vorticity logarithmic gradient is therefore:

$$\frac{d\log(\Sigma/B)}{d\log r} = \frac{r}{\lambda}\log\left(\frac{\Sigma_o}{\Sigma_i}\right)\left(a + b\frac{H^2}{\lambda^2}\right), \tag{10}$$

where a and b are numerical functions of r of order unity that depend on the exact shape of the surface density profile. In particular, one sees immediately that if $\lambda \sim H$, the contributions of both terms (the surface density gradient and the vorticity gradient) to the corotation torque are of similar magnitude.

The corotation torque at the transition Γ'_C can therefore be larger than the corotation torque Γ_C further out in the disk by a factor:

$$\frac{\Gamma'_C}{\Gamma_C} \approx \frac{2r}{3\lambda} C, \tag{11}$$

where C is a numerical factor of order unity that depends on the surface density profile.

Using Eqs. (3), (5) and (11), we find that:

$$\frac{\Gamma'_C}{\Delta\Gamma'} \approx -\frac{8H}{3\lambda} C, \tag{12}$$

which means that the (positive) corotation torque can counteract the (negative) Lindblad torque at a cavity, provided that the edge of the latter be narrow enough ($\lambda < 8HC/3$). We check by means of numerical simulations that it is indeed possible to halt type I migration on the edge of a surface density transition.

3. Numerical set up

We performed a large number of two-dimensional hydrodynamical simulations that we detail below. The code used was FARGO[1]. It is a staggered mesh code on a polar grid, with upwind transport and a harmonic, second order slope limiter (van Leer 1977). It also uses a change of rotating frame on each ring that enables one to increase significantly the time step (Masset 2000a,b).

The surface density transition was set in the following manner. We call F the target surface density ratio between the inside and the outside of the cavity: $F = \Sigma_o/\Sigma_i$. In order to realize this ratio, we adopt a fixed profile of kinematic viscosity with an inverse ratio: $\nu_o/\nu_i = F^{-1}$. If we call r_t the mean radius of the transition, then for $r > r_t + \lambda/2$, $\nu \equiv \nu_o$, for $r < r_t - \lambda/2$, $\nu \equiv \nu_i$, and for $r_t - \lambda/2 < r < r_t + \lambda/2$, ν is an affine function of r. We then relax the surface density profile during a preliminary 1D calculation over $\sim 10^5$ orbits, so that the profile can safely be considered as steady state in the 2D calculations. In our

[1]See: `http://www.star.qmul.ac.uk/~masset/fargo`

calculations we use non-reflecting inner and outer boundary conditions, while we impose the disk surface density at the inner and outer boundary.

In all our calculations the disk aspect ratio is $h = 0.05$, the disk is not self-gravitating and it has a locally isothermal equation of state. The length unit is r_t. The mesh inner and outer boundaries are respectively at $r = 0.42$ and $r = 2.1$. The mass unit is the mass M_* of the central object, and the gravitational constant is $G = 1$. The time unit is $(GM_*/r_t^3)^{-1/2}$. Whenever we quote a planet mass in Earth masses, we assume the central object to have a solar mass.

The mesh size in all our runs is $N_r = 168$ and $N_\phi = 450$, hence the radial resolution is 10^{-2}. The horseshoe zone width for a 15 $M_\oplus$ planet is $\sim 7.8 \cdot 10^{-2}$, so it is ~ 8 zones wide. The error on the corotation torque due to this finite width therefore amounts to at most ~ 10 % [see Masset (2002), Fig. A.3]. We also made calculations with a 4 $M_\oplus$ mass planet for which the horseshoe zone is only 4 zones wide. This resolution may seem low but the corotation torque is very well captured at low resolution for small mass planets which hardly perturb the surface density profile [see discussion in Masset (2002), Appendix A].

We contemplated the fashionable issue of whether the Roche lobe content must be included or not when integrating the torque over the disk material (D'Angelo et al. 2005; Masset & Papaloizou 2003). We found that taking that material into account or not makes essentially no difference in our case. We make the following technical comments related to this issue:

- D'Angelo et al. (2005) have envisaged the case of Jupiter or Saturn mass planets, for which there is a significant Roche lobe with radius $\sim a(M_p/3M_*)^{1/3}$ (a being the planet semi-major axis). For the mass range studied here ($M_p < 15\ M_\oplus$), the Roche lobe size is much smaller than this simple estimate. In particular, in the linear limit, the flow does not exhibit any circumplanetary libration, while the two ends of the horseshoe region reconnect through a single stagnation point located on the orbit (Masset et al., in prep.; Tanaka, private communication), that is offset from the planet as a result of the gaseous disk slight sub-Keplerianity. The issue of Roche lobe sampling in that case is therefore irrelevant.

- D'Angelo et al. (2005) have found that resolution may alter the torque exerted on the planet when the Roche lobe material is taken into account. This behavior, which appears at very high resolution, is related to the build up of a gaseous envelope around the point-like planet, while the mass of this envelope heavily depends upon the equation of state, which is poorly known. The envelope mass may be considerable for the giant protoplanets considered by D'Angelo et al. (2005), as it may be several times the planet

mass, but it is presumably a much smaller fraction of the planet mass for the planet masses that we consider [$M_p < 15\ M_\oplus$; see also Alibert et al. (2005)].

In 2D simulations one has to introduce a potential smoothing length ϵ meant to mimic the disk vertical extent. The planet potential expression is then $-GM_p/(r^2+\epsilon^2)^{1/2}$, where G is the gravitational constant and r the distance to the planet. In our calculations we use a potential smoothing length $\epsilon = 0.7H$. This is quite a large value, which leads to underestimate the corotation torque (Masset 2002), as it lowers the horseshoe zone width, while the corotation torque is proportional to the fourth power of this width. Our calculations are therefore conservative, and it is likely that 3D calculations would yield a torque cancellation for an even wider set of disk parameters than what we found.

4. Results of numerical simulations

4.1. Torque sampling on a cavity edge

We consider in this section a disk with a target surface density ratio between the inside and the outside of the transition set to $F = 7$. As this value is large compared to one, we call the inside part of the transition a cavity. We performed two sequences of 75 calculations in which a planet was set on a fixed circular orbit with radius $a_i = 0.65 + 10^{-2} i$ ($i = 0 \ldots 74$). For these calculations we report as a function of a_i the total torque exerted on the planet [averaged over 100 orbits, in order for the libration flow inside the co-orbital region to reach a steady state (Masset 2002)].

The left plot of Fig. 1 shows the relaxed surface density profile after 10^5 orbits of the preliminary 1D calculation, and the right plot shows the quantities involved in the corotation torque scaling. The right panel of Fig. 1 shows that the vortensity gradient peak is only partially due to the surface density gradient, since the gradient of the flow vorticity plays a role of comparable importance, as suggested in section 2.

The total torque measured from numerical simulations is presented on Fig. 2. Both plots, which correspond to two different planet masses, exhibit similar features:

- On the left side (for $r < 0.8$) and on the right side (for $r > 1.2$), the torque profile is flat and negative. This corresponds to the total negative torque acting on a planet embedded in a flat surface density disk. Since the surface density is $F = 7$ times lower on the inside, the torque value is much smaller on that side.
- In the range $0.8 < r < 1.2$, the torque as a function of radius exhibits a shape very

similar to the vortensity gradient shown on Fig. 1. In particular the torque has a maximum value near $r = 1.08 - 1.10$ and a minimum value near $r = 1.12 - 1.13$.

This last observation unambiguously indicates that the corotation torque largely dominates the total torque at the surface density transition, as expected from the analytic estimate. In particular, there are two positions in the disk where the total torque cancels out (and therefore where the migration is halted): one at $r \approx 0.92$ and the other one at $r \approx 1.11-1.12$. The first of these fixed points is unstable : moving the planet away from it yields a torque that moves it further away, while the second one (i.e. the outermost one) is stable: moving the planet to a higher radius yields a negative torque that tends to bring the planet back to its former position, and vice-versa for a motion towards smaller radii. The fixed point at $r = 1.12$ should therefore trap all type I migrating embryos. We note in passing that the torque as a function of radius does not have exactly the same shape between a 15 $M_\oplus$ and a 4 $M_\oplus$ planet. There are two reasons for this: the onset of non-linear effects between 4 $M_\oplus$ and 15 $M_\oplus$, and the inaccuracy of the corotation torque estimate for the 4 $M_\oplus$ case, for the resolution that we have adopted. However, we see that even in the 4 $M_\oplus$ case, the value of the torque maximum ($\sim 6 \cdot 10^{-5}$) is much larger than the torque absolute value away from the cavity (for $r > 1.2$, this value is $\sim 10^{-5}$). Therefore, even if the error on the corotation torque amounts to 50 % [see Masset (2002)], one still gets a torque cancellation and a stable fixed point.

4.2. Halting migration at a cavity edge

We have performed a series of ten calculations with planets of masses 1.3 $M_\oplus$ to 15 $M_\oplus$ in geometric sequence, with the same disk cavity as in the previous section ($F = 7$). In these calculations the planets were released at $r = 1.35$, i.e. beyond the cavity edge, and then allowed to freely migrate under the action of the disk torque. The results are presented at Fig. 3. We see how the transition efficiently traps all these objects at the fixed point at $r = 1.12$ identified at the previous section. We note in passing that on the lower side of the mass range considered, the small width of the horseshoe region may lead to large uncertainties on the corotation torque. Nevertheless, the migration of all objects stops at locations which are all very close to 1.12. This indicates that the corotation torque at the edge, even misrepresented by a too low resolution, still strongly dominates the differential Lindblad torque. For masses lower than a few earth masses, the Hill radius is much smaller than the disk thickness and the disk response is linear. In the linear regime, the corotation to Lindblad torque ratio is independent of the planet mass. As we have stressed already, our potential smoothing length is large and our corotation torque estimate is conservative. This

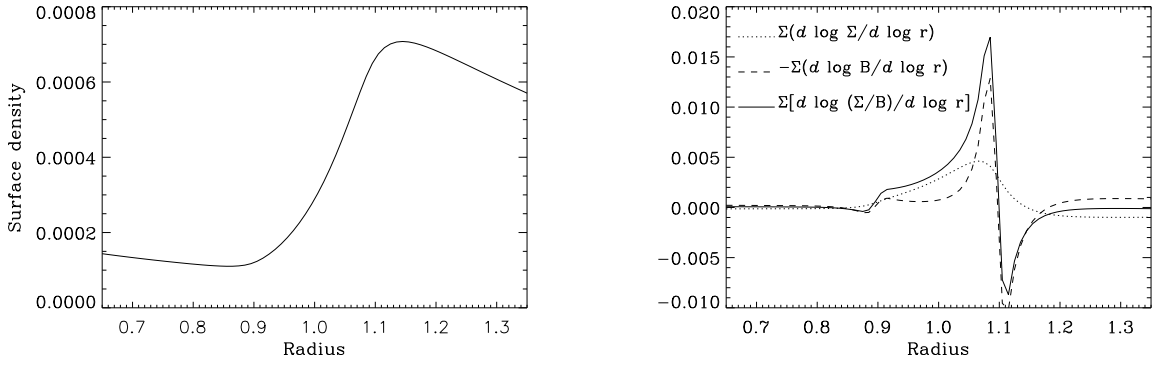

Fig. 1.— Left: surface density profile for the runs of section 4.1. The surface density transition occurs over $\sim 4H$, between $r \approx 0.9$ and $r \approx 1.1$. Right: Corresponding profiles of the different logarithmic derivatives involved in the expression of the corotation torque, weighted by the surface density. The dotted line shows the logarithmic derivative of the surface density, the dashed line shows the opposite of the logarithmic derivative of the flow vorticity, and the solid line shows the sum of these two quantities. It corresponds to the R.H.S. of Eq. (4).

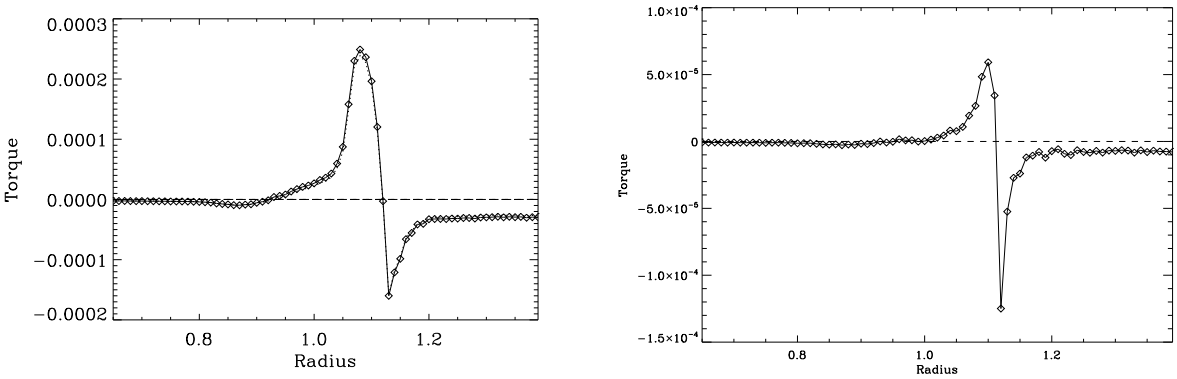

Fig. 2.— Left: Specific torque acting upon a 15 $M_\oplus$ planet on a fixed circular orbit, as a function of its orbital radius. Right: same thing for a 4 $M_\oplus$ planet.

indicates that any small mass in-falling embryo will be trapped at the cavity edge that we modeled.

Disk profiles with an extremum of the specific vorticity are prone to a linear Rossby wave instability that eventually leads to the formation of vortices (Li et al. 2000, 2001). This is the case of the transitions that we have simulated. The arc-shaped over-dense region located near $x = -0.5, y = +0.5$ in the right plot of Fig. 3 corresponds to such a vortex. It leads to a torque modulation over the synodic period between the planet and the vortex, that is seen on the migration curves of the left plot of Fig. 3. As a planet approaches the transition, the synodic period increases, and so does the period of the semi-major axis modulations.

4.3. Torque sampling at a shallow surface density jump

We have performed a series of calculations similar to those of section 4.1, except that we adopted a much smaller target outer to inner surface density ratio: $F = 1.4$ instead of 7. The surface density jump is therefore a very shallow one. The results are presented on Fig. 4. They show that again there is a fixed point at which migration is halted, at $r \approx 1.09$. We have not searched further the limit inner to outer surface density ratio that leads to migration reversal, as this quantity depends on the jump radial size, on the profile adopted for the kinematic viscosity and on the potential smoothing length. We just stress that a factor $F = 1 + O(1)$ and a jump size of $\sim 4H$ suffices to halt migrating bodies.

4.4. Driving of trapped planets

As can be seen on Fig. 2 or 4, the torque maximum value is positive and large. This implies that, if the cavity radius evolves with time, either inwards or outwards, it drives any planet trapped on its edge so that its migration follows the edge evolution. More precisely, a planet will be held at a location where the specific torque acting upon it endows it with a drift rate equal to that of the cavity radius. As the torque maximum in absolute value is at least of the order of the total torque in the outer disk, this means that the edge expansion or contraction can be as fast as the type I drift rate of its trapped objects and still keep these objects trapped. We illustrate this shepherding on Fig. 5. We performed a calculation in which an initially fixed cavity such as the one considered at the previous sections (here with $F = 10$ and a transition over $4 - 5H$) traps a 15 $M_\oplus$ in-falling planet and then is endowed with an expansion rate $\dot{r}_t = 8 \cdot 10^{-5}$. This is achieved by imposing a kinematic viscosity profile as described in section 3 with a radius r_t that varies linearly with time. One can

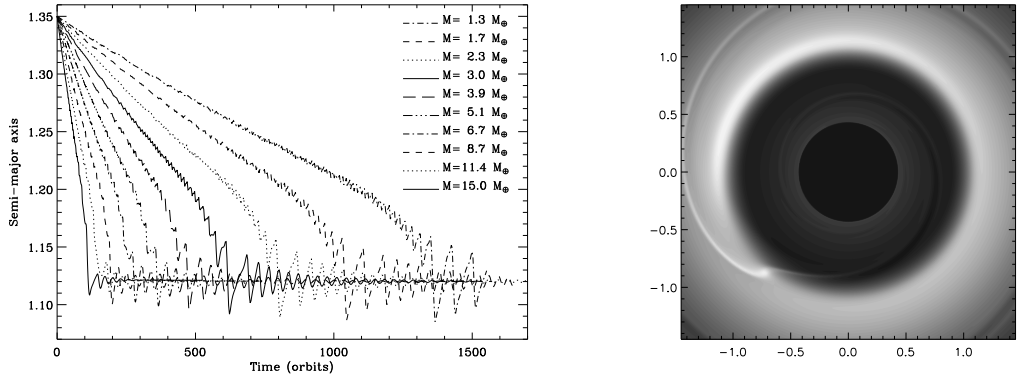

Fig. 3.— Left plot: primary to planet separation curve as a function of time, for the 10 different planet masses. Right plot: snapshot of the surface density map with a 15 $M_\oplus$ planet embedded at $t = 480$ orbits.

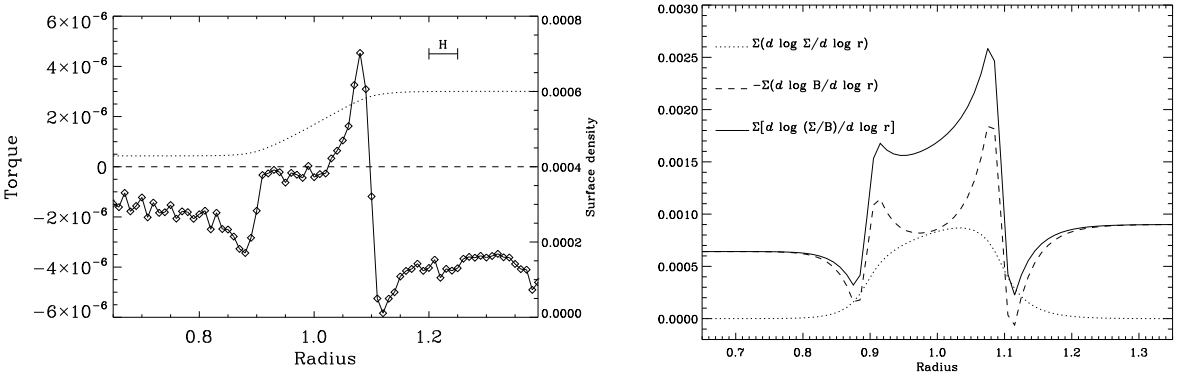

Fig. 4.— Left: surface density profile for the runs of section 4.3 (dotted line and right axis) and total torque exerted by the disk on the planet as a function of its semi-major axis (diamonds and left axis), for a 4 $M_\oplus$ planet. Right: Corresponding profiles of the different logarithmic derivatives involved in the expression of the corotation torque, weighted by the surface density, as in Fig. 1.

see that the planet semi-major axis follows the cavity radius evolution, so that the planet remains trapped on the cavity edge.

4.5. Dissipation and corotation torque saturation

4.5.1. Corotation torque saturation

The corotation torque, in the absence of any angular momentum exchange between the horseshoe region and the rest of the disk, is prone to saturation: its value tends to zero after a few libration periods (Ward 1991, 1992; Masset 2001; Balmforth & Korycansky 2001; Masset 2002). The disk turbulence, which endows the disk with an effective viscosity, can help to prevent the corotation torque saturation. Here we estimate the amount of viscosity required to prevent saturation, as a function of the planet mass. The maximal amount of saturation for which one still has a torque cancellation depends on the planet mass and on the detailed disk profiles. Here we just give an order of magnitude of the viscosity needed to prevent saturation by assuming a 50 % saturation. This amount of saturation is reached when the viscous timescale across the horseshoe region is equal to the horseshoe libration timescale (Masset 2001):

$$\frac{x_s^2}{3\nu} = \frac{4\pi a}{(3/2)\Omega_p x_s}, \tag{13}$$

where x_s is the horseshoe zone half width, ν is the disk effective kinematic viscosity, Ω_p is the planet orbital frequency and a its semi-major axis. In order to express x_s as a function of the planet mass[2], we note that in the linear (hence fully unsaturated) limit the corotation torque can be expressed as (Ward 1991; Masset 2001):

$$\Gamma_C = \frac{9}{8} x_s^4 \Omega_p^2 \Sigma, \tag{14}$$

while from Tanaka et al. (2002) we have:

$$\Gamma_C = 0.939 h^{-2} q^2 a^4 \Omega_p^2 \Sigma, \tag{15}$$

where $q = \frac{M_p}{M_*}$. Eqs. (14) and (15) yield:

$$x_s = 0.96 a \sqrt{\frac{q}{h}}. \tag{16}$$

[2]The estimate provided here is given for a flat surface density profile, but the horseshoe region width should not or very weakly depend on this assumption.

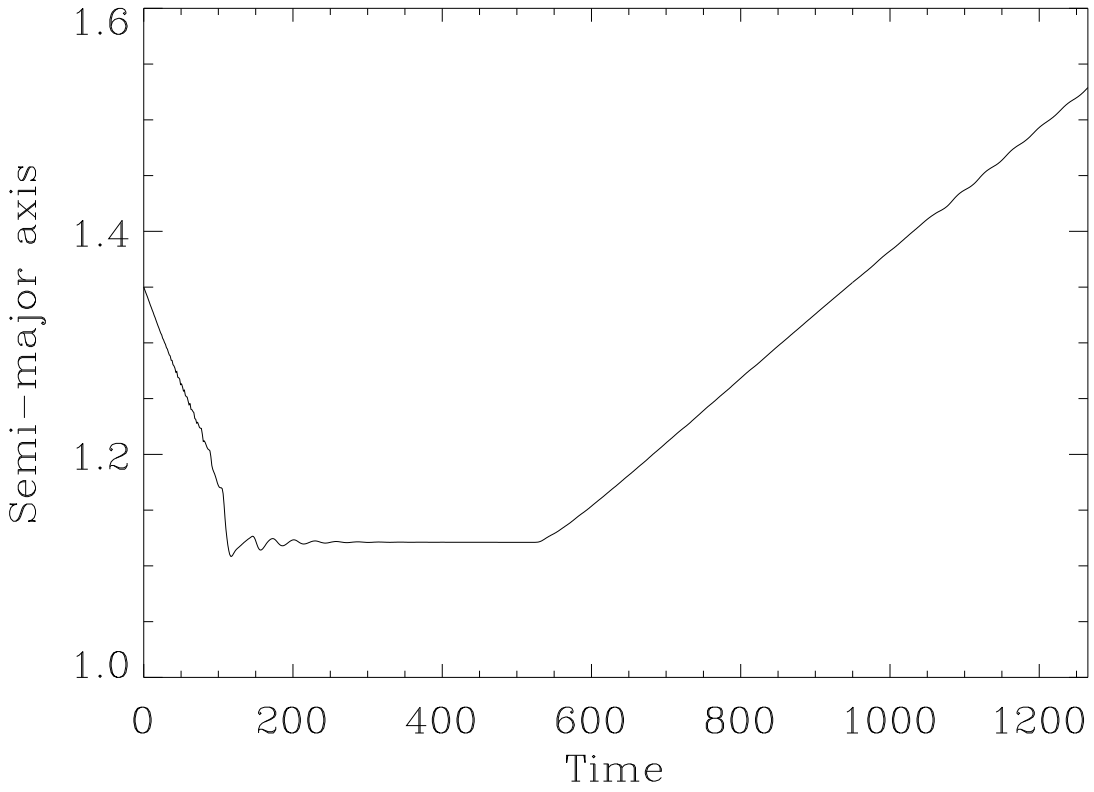

Fig. 5.— Semi-major axis as a function of time for a planet trapped in an expanding cavity. The cavity is fixed for the first 520 orbits, then is linearly expanding with time. The planet semi-major axis follows the cavity evolution so that the planet remains trapped at the cavity edge. At $t = 0$ the planet is released beyond the cavity, at $r = 1.35$. During the first 100 orbits it migrates towards the cavity where it gets trapped.

Eqs. (13) and (16) give the minimum effective viscosity to prevent the corotation torque saturation:

$$\nu = 0.035 \left(\frac{q}{h}\right)^{3/2} a^2 \Omega_p, \tag{17}$$

or, in terms of the α coefficient ($\nu = \alpha H^2 \Omega_p$):

$$\alpha = 0.035 q^{3/2} h^{-7/2} = 6.5 \cdot 10^{-6} \cdot \left(\frac{M_p}{1\ M_\oplus}\right)^{3/2} \cdot \left(\frac{h}{0.05}\right)^{-7/2} \tag{18}$$

The value of α required to prevent the corotation torque saturation of an Earth mass planet is therefore much smaller than the one inferred from disk lifetimes of T Tauri stars, namely $\alpha = 10^{-3} - 10^{-2}$ (Hartmann 2001). Note that this also holds for large mass solid cores ($M_p = 10 - 15\ M_\oplus$). The corotation torque acting on these objects should therefore be a large fraction of the unsaturated estimate, so the analysis presented above for the torque cancellation is essentially valid. We also note that the planets of Figs. 3 and 5 remain trapped over a timescale much longer than the horseshoe libration timescale, so that their corotation torque partial saturation is weak enough. The disk effective viscosity at the trap location is in these calculations $5 \cdot 10^{-6}$ (i.e. $\alpha = 2 \cdot 10^{-3}$).

We comment that the corotation torque saturation could be different in a laminar disk with kinematic viscosity ν and in a turbulent disk (we discuss more in detail this topic in the next section) with the same effective viscosity, when the horseshoe region width is smaller than the turbulence length scale. The saturation should be easier to remove in this last case, which suggests that our saturation estimates is a conservative one.

4.5.2. Dissipation and turbulence

Since the likely physical origin of the disk effective viscosity is turbulence, in particular the turbulence generated by the magneto-rotational instability (MRI) (Balbus & Hawley 1991), the torque acting upon the planet does not have a value constant in time as in a laminar disk, but rather displays large temporal fluctuations arising from the density perturbations in the planet vicinity. It is important to assess the impact of these fluctuations on the mechanism outlined here. In the bulk of a disk with a smooth surface density profile, these torque fluctuations can yield an erratic behavior of the planet semi-major axis referred to as "stochastic migration" (Nelson & Papaloizou 2004; Nelson 2005). In what follows we use the torque fluctuation estimates of Nelson & Papaloizou (2004) and Nelson (2005) in order to determine whether despite of its semi-major axis jitter the planet is confined to the trap vicinity, or whether it is unlocked the from the trap position. We use a very simple prescription, that we detail in appendix A, to perform Monte-Carlo calculations of the planet

semi-major axis over a period of time $t = 10^7\ \Omega^{-1}$. We place initially the planet at the outer stable fixed point, and we declare it trapped if over that amount of time it never goes through the inner, unstable fixed point, while we declare it not trapped if it happens to go through the inner fixed point. While appendix A presents the technical details of our calculations, we discuss below a number of issues relevant to these calculations.

- Can the torque acting upon the planet be considered as the sum of the torque in a laminar disk and the fluctuations arising from turbulence ? Nelson (2005) finds that this might not be the case, at least as long as the differential Lindblad torque is concerned, since the corotation region is not sufficiently resolved in his calculations; as an alternative explanation to the lack of the torque convergence to the laminar value, Nelson (2005) suggests the existence of very low frequency components of the torque fluctuations. As this problem is essentially open (and totally unaddressed as far as the corotation torque is concerned), we chose to describe the torque acting upon the planet by the sum of the torque in the laminar case and of the torque fluctuations due to the turbulence.

- The amplitude $\mathcal{A}$ of the torque fluctuations can be estimated by considering a density fluctuation of order unity with a length scale of order H, at a distance H from the planet (Nelson & Papaloizou 2004; Nelson 2005) and found to amount to $\mathcal{A} = G\Sigma r$, where G is the gravity constant and r the distance to the central object. This is the value that we adopt for our calculations.

- The time scale of the fluctuations is of particular importance to assess the torque convergence towards its laminar value. Nelson (2005) finds in his calculations that the torque fluctuations due to turbulence contain significant power at very low frequency, and suggests that this could be linked to global communication across the disk on the viscous timescale. Here our situation is rather different, as the planet lies on a radially localized structure, with a radial extent λ. Fluctuations with frequency lower than $\sim \lambda/c_s$ would imply turbulent structures larger than the trap width, and therefore would imply a radial displacement of the trap itself along the lines of section 4.4. Here we choose a correlation timescale for the turbulence of $t_c = 8\Omega^{-1} \sim 2\lambda/c_s$ for $\lambda \sim 4H$.

- Both the tidal torque and the torque fluctuations scale with the disk surface density, so that the time needed for the time averaged torque to reach convergence does not depend on the latter. However, the spread of the probability density of the planet semi-major axis after that timescale does depend on the disk surface density. If the expectancy of the distance of the planet to its initial location is larger than the trap width, then the planet can certainly be lost, while if it is much smaller than the trap width, the planet

is certainly trapped. Our study therefore amounts to a disk critical mass search. For a given trap profile, a given planet mass and given fluctuation characteristics $\mathcal{A} \propto \Sigma$ and t_c, there exists a critical disk mass so that a lighter disk keeps the planet trapped, while a heavier disk is unable to lock it and the planet is likely to go through the inner unstable fixed point. We perform this search in a dichotomic manner until we reach a precision of 5 % on the disk mass, and we repeat the calculation with different random seeds, so as to get an idea of the precision on the disk critical mass estimate. Our results are displayed on Fig. 6. The "disk outer mass" is defined as $M_{\rm outer\ disk} = \pi r_t^2 \Sigma_{\rm out}$, where $\Sigma_{\rm out}$ is the disk surface density on the outside of the surface density transition. We see on this figure that the deep cavity with $F = 7$ unconditionally traps $M = 1$ to 15 $M_\oplus$ protoplanets in a disk with a density profile of the minimum mass solar nebula, at any distance up to ~ 5 AU, while the shallow surface density transition would be able to retain in falling bodies only in the very central regions ($r_t \simeq 0.01$ AU, if the nebula extends that far in) of such a nebula. Further out in the disk, at $r = 0.1$ AU, a shallow transition in the MMSN would only capture embryos with $M > 4\ M_\oplus$, etc.

It is not unreasonable to assume that these simple calculations are conservative, for the following reasons:

- We have assumed the torque fluctuations to scale only with the disk surface density, which implies that all the disk material in the trap vicinity is turbulent. There is at least one realization of the trap, which is the inner edge of a dead zone (detailed at the next section), for which this statement is wrong. In our example, the trap stable fixed point corresponds to a location with a large surface density, therefore located rather on the "dead" side of the transition, i.e. where turbulent transport of angular momentum is inefficient and hence where the turbulence should be much weaker than contemplated in our simple Monte Carlo calculations.

- We recall that our large potential smoothing length tends to significantly underestimate the corotation torque, while the trap ability to lock infilling bodies, for a given turbulence characteristics, strongly depends on the corotation torque peak value at the surface density transition.

We conclude this section with two remarks. Firstly, the numerical simulations undertaken by Nelson & Papaloizou (2004) and Nelson (2005) neglect, for reasons of computational speed, the gravitational potential z dependency, which means that their disks have no vertical stratification. Future numerical experiments with vertical stratification may lead to different characteristics of the torque fluctuations. Secondly, other sources of turbulence have been

suggested in protoplanetary disks, such as the global baroclinic instability (Klahr 2004), which may have different torque fluctuations statistics, and for which the trap efficiency may therefore be different. To date this is essentially an unaddressed issue.

5. Discussion

The mechanism exhibited here is generic, since it plays a role at any positive disk surface density transition, even shallow ones, with the cautionary remark that some turbulence is required to prevent the corotation torque saturation, and that a condition is required on the disk mass to prevent the stochastic migration induced by the turbulence to overcome the trap effect. Although our knowledge of the detailed properties of protoplanetary disks is still incipient, we already know a number of locations for transitions exhibiting the above properties, which constitute potential traps for in-falling embryos:

- At the inner edge of a dead zone (Gammie 1996; Fromang et al. 2002), the surface density is expected to be significantly larger in the dead zone than in the ionized inner disk, while the inner disk turbulence provides the dissipation required to maintain the corotation torque. If the dead zone inner radius changes with time (since layered accretion involving a dead zone is thought not to be a steady process) the objects trapped at the fixed point follow the transition radius, as shown in section 4.4. The edges of dead zones are thought, in the totally different context of runaway or type III migration (Masset & Papaloizou 2003), to be able to halt or reverse a runaway episode (Artymowicz 2004). Here, in our context of small mass, type I migrating objects, we argue that the inner edge of a dead zone halts type I migrating bodies and efficiently traps them.

- Sizable surface density transitions can also be found at the transition between an inner disk region where jets are launched and the outer viscous disk (Ferreira & Pelletier 1995). Indeed, the accretion velocity in the jet emitting disk (hereafter JED) region is entirely due to the jet torque and becomes much larger than in a standard accretion disk (hereafter SAD). Mass flux conservation then leads to a surface density jump at the transition radius between the SAD and the JED. This radius has been inferred to vary from 0.3 to a few astronomical units in some T Tauri stars[3] (Coffey et al. 2004;

[3]In fact, velocity shifts detected in jets are interpreted as being a rotation signature which then allows one to derive the outer jet launching radius in the underlying accretion disk. This radius corresponds to our transition radius.

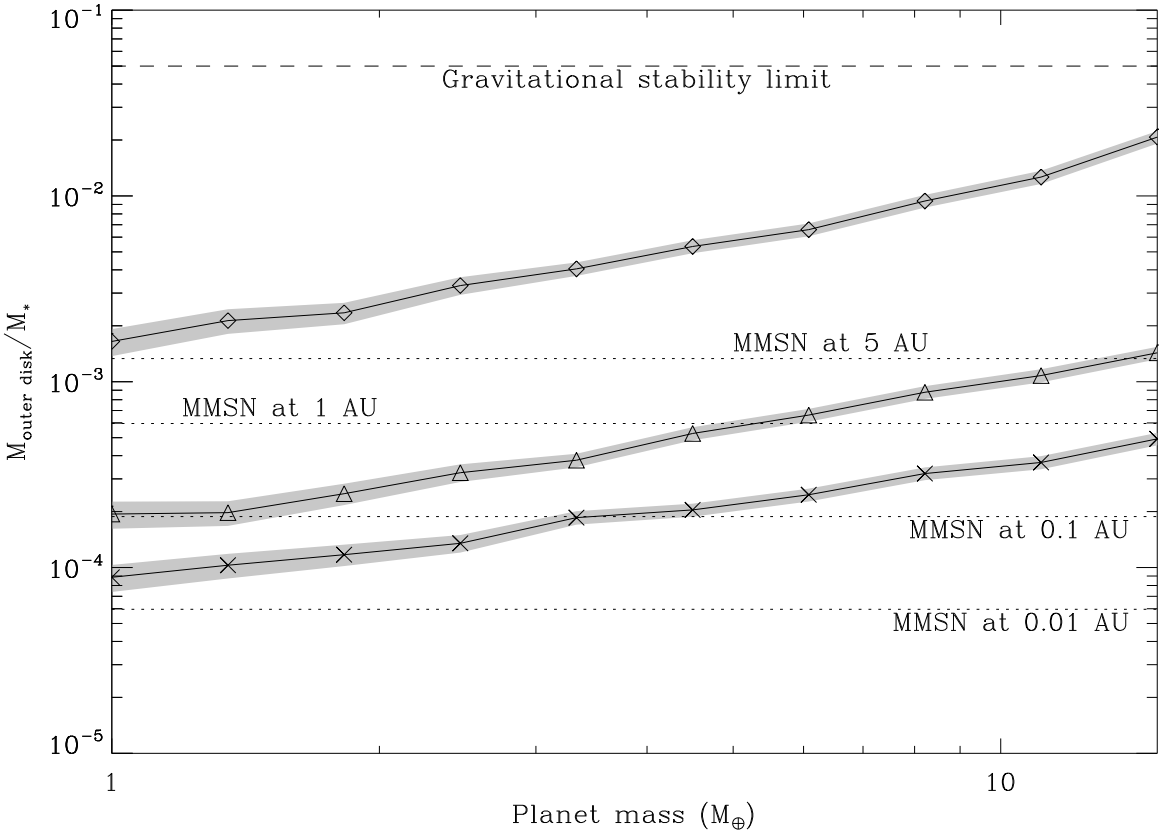

Fig. 6.— Critical disk mass as a function of the planet mass (from 1 $M_\oplus$ to 15 $M_\oplus$), for different transition profiles: the $F = 7$ cavity of section 4.1 (diamonds), the $F = 1.4$ shallow jump of section 4.3 (crosses). The triangles represent the trapping limit for a torque curve with a peak maximum which is the geometric mean of the peak values of the $F = 7$ and $F = 1.4$ transitions, which we assume to be representative of a transition with $F \simeq 1 + \sqrt{0.4 \times 6} = 2.5$. The dotted lines show the minimum mass solar nebula relative mass (as defined by its local surface density) at different radii. The thickness of the gray line indicates the results standard deviation found with different random seeds.

Pesenti et al. 2004). As all known embedded objects have jets, the existence of such a transition radius provides a natural trap for in-falling embryos over the jet lifetime.

- We finally mention the outer edge of a gap opened by a preexisting giant protoplanet. The latter can trap planetesimals at mean motion resonances (Hahn & Ward 1996), but also at the large positive surface density gradient found on its gap outer edge.

We note that the first two possibilities might not coexist in an accretion disk. Not all T Tauri stars show indeed evidence of high velocity jets (Hartigan et al. 1995). For these jet-less stars, the whole disk is likely to resemble a SAD with a dead zone in its innermost region. The protoplanet trap would then be realized at the inner radius of the dead zone, namely only if there is a SAD settled at smaller radii. Objects with a dead zone extending down to the star would have no trap. On the contrary, young stars producing jets require the presence of a JED in the inner disk region. In that case, the trap is located at the outer JED radius (the JED itself may extend down to the star with no impact on the trap). Note also that since a JED is less dense than a SAD, it is unlikely that a dead zone would establish (Ferreira et al. in prep.).

The likely existence of such planetary traps in protoplanetary disks has important implications for the formation of giant planets. First, it constitutes a workaround to the timescale conflict between a solid core build up (which is slow) and its migration to the central object (which would be fast, if the object was not stopped at a trap). Second, a large amount of solid embryos should accumulate at the trap location. This should speed up the build up of a critical mass core ($M_p \simeq 15\ M_\oplus$) which could accrete the nebula gas and convert itself into a giant planet. The dynamics of the set of embryos trapped at the jump is however beyond the scope of this communication, and will be presented in a forthcoming work.

We have seen in section 2 that the corotation torque value is boosted not only by the large surface density gradient but also by the alteration of the rotation profile, which yields a large gradient of B, with both large minimal and maximal values since the gradient of B involves the second derivative of the angular velocity. One may wonder whether at a disk opacity transition, in which there is a disk temperature jump and hence a pressure gradient radial jump, the alteration of the rotation profile is sufficient to yield a peak value of the corotation torque that counteracts the Lindblad torque. We have undertaken subsidiary calculations in which we have a power law surface density profile and a sound speed profile with a localized radial jump. We found that we need a jump of the aspect ratio of ~ 1.5 over $4H$ in order to halt migration. This ratio is too large and is unrealistic in a SAD. Indeed, in a standard accretion disk in which energy is transported vertically by radiative diffusion, the central temperature scales as $\tau^{1/8}$, where τ is the optical depth. As a consequence, even

in the vicinity of an opacity transition, the temperature profile exhibits a smooth behavior and the corotation torque is not sufficiently strong to counterbalance the Lindblad torque. Nevertheless, Menou & Goodman (2004) have found that the opacity transitions may induce a significant reduction of the differential Lindblad torque, but they explicitly neglected the corotation torque in their study. It would be of interest to investigate whether the corotation torque boost at these locations can be sufficient to halt migration.

Remarkably, the scale height of a JED is always smaller than that of the SAD, so that the transition between these two flows naturally yields a jump in the disk aspect ratio. This is due to two effects. First, a JED feeds its jets with most of the released accretion power so that only a small fraction of it is radiated away at the disk surface: the disk is cooler. Second, in addition to gravity, the large scale magnetic field vertically pinches the disk (Ferreira 1997).

We also stress that at the inner dust puffed-up rims of protoplanetary disks (Isella & Natta 2005), there can be a large radial gradient of the gas temperature, which may be sufficient to trap migrating planets.

We finally emphasize that the mechanism presented here does not allow low mass objects to proceed inside of a cavity, but rather traps them on the cavity edge. This is quite different from what has been studied in the context of gap opening planets, which migrate further inside until they reach the $2:1$ resonance with the cavity edge (Kuchner & Lecar 2002).

6. Conclusions

We have shown that the type I migration of $M_p < 15 M_\oplus$ planets can be halted at radially localized disk surface density jumps (the surface density being larger on the outside of the jump). Some turbulence is then required to prevent the corotation torque saturation. The latter tends to induce stochastic migration of the embryos, and therefore tends to act against the trap. The lighter the disk, the easier it is to keep an embryo trapped, since its radial jitter over the timescale needed to reach torque convergence is small and can be confined to the vicinity of the trap stable fixed point. Inversely, the lighter the embryo, the more difficult it is to trap it: in the zero mass limit, the embryo has no tidal torque and only feels the torque fluctuations arising from turbulence. We have shown that a jump with a large surface density ratio efficiently traps embryos above one Earth mass up even in relatively massive disks, such as the MMSN at $r = 5$ AU, while shallow jumps (a 40 % surface density increase over ~ 4 disk scale heights) will retain embryos of a few Earth masses and more only in light disks, such as the MMSN at $r = 0.1$ AU. We have illustrated by means

of numerical simulations that a surface density jump traps in-falling embryos, and that it drives them along with it if it moves radially as the disk evolves. Such a jump can occur at different locations in a protoplanetary disk: it can be found at the transition between the standard accretion disk solution (SAD) and the jet emitting disk (JED), thought to be at a distance 0.3 to $1-2$ AU from the central object. It can also be found at the inner edge of a dead zone, where one expects a very large ratio of outer to inner surface densities. It may also be found at the outer edge of a protoplanetary gap if one giant planet already exists in the disk. We have stressed that these planetary traps have two important consequences: (i) they can hold the type I migration of protogiant cores over the timescale needed to overcome the critical mass ($\sim 15\ M_\oplus$) over which rapid gas accretion begins onto these cores, which are then quickly converted into giant planets that should enter the slow, type II migration regime; (ii) as solid embryos accumulate at the trap, the build up of critical cores should be faster than elsewhere in the disk. Finally, we mentioned that although temperature radial jumps in principle also yield large peaks of the corotation torque, they are unlikely to be able to counteract the Lindblad torque by themselves, as the temperature gradients required for that are unrealistically large in a standard accretion disk.

A. Prescription for the 1D calculation of the planet semi-major axis time evolution in the presence of torque fluctuations

The planet semi-major axis is evolved in time using an Euler method:

$$a(t+\Delta t) = a(t) + \Delta t \frac{\Gamma_l + \Gamma_f}{2B[a(t)]a(t)}, \tag{A1}$$

where $a(t)$ is the planet semi-major axis at date t, Γ_l is the torque as measured in a laminar disk for a planet in circular orbit of radius a, linearly interpolated from the results displayed either in fig. 2a or 4a, Γ_f is the torque fluctuation due to turbulence, and where a Keplerian profile is assumed for B (this is grossly wrong as far as its radial derivative is concerned, as we saw in the main text, but this is largely sufficient for our purpose here). The torque fluctuation is evaluated as follows:

$$\Gamma_f = G\Sigma_m[a(t)]a(t)[2V-1], \tag{A2}$$

where $\Sigma_m[a] = \max[\Sigma(r)]_{r\in[a-H,a+H]}$, and where V is a random variable uniformly distributed over $[0,1]$. The value of Γ_f is kept constant over t_c. We use the above prescription for $\Sigma_m[a]$ since the planet is located in a region where the surface density gradient is large. The largest torque fluctuations may arise from regions located within $a-H$ to $a+H$ from the central object, and where the surface density may be significantly different from the one at the

planet location. Each realization of the random variable is independent of the previous ones. We anticipate that the results should not depend on the torque fluctuation law, since the Central Limit Theorem states that the cumulative torque law tends towards a normal law (Nelson 2005).

REFERENCES

Alibert, Y., Mordasini, C., Benz, W., & Winisdoerffer, C. 2005, A&A, 434, 343

D'Angelo, G., Bate, M. R., & Lubow, S. H. 2005, MNRAS, 358, 316

Artymowicz, P. 2004, ASP Conf. Ser. 324: Debris Disks and the Formation of Planets, 324, 39

Balbus, S. A., & Hawley, J. F. 1991, ApJ, 376, 214

Balmforth, N. J., Korycansky, D. G. 2001, MNRAS, 326, 833

Coffey, D., Bacciotti, F., Woitas, J., Ray, T. P., & Eislöffel, J. 2004, ApJ, 604, 758

Ferreira, J. 1997, A&A, 319, 340

Ferreira, J., & Pelletier, G. 1995, A&A, 295, 807

Fromang, S., Terquem, C., & Balbus, S. A. 2002, MNRAS, 329, 18

Gammie, C. F. 1996, ApJ, 457, 355

Goldreich, P., & Tremaine, S. 1979, ApJ, 233, 857

Hartigan, P., Edwards, S., & Ghandour, L. 1995, ApJ, 452, 736

Isella, A., & Natta, A. 2005, A&A, 438, 899

Hahn, J. M., & Ward, W. R. 1996, Lunar and Planetary Institute Conference Abstracts, 27, 479

Hartmann, L. 2001, in Accretion Processes in Star Formation, Cambridge University Press

Klahr, H. 2004, ApJ, 606, 1070

Korycansky, D. G., & Pollack, J. B. 1993, Icarus, 102, 150

Kuchner, M. J., & Lecar, M. 2002, ApJ, 574, L87

Li, H., Finn, J. M., Lovelace, R. V. E., & Colgate, S. A. 2000, ApJ, 533, 1023

Li, H., Colgate, S. A., Wendroff, B., & Liska, R. 2001, ApJ, 551, 874

Lin, D. N. C., & Papaloizou, J. 1986, ApJ, 307, 395

Lin, D. N. C. & Papaloizou, J. C. B. 1986, ApJ, 309, 846

Masset, F. S. 2002, A&A, 387, 605

———. 2001, ApJ, 558, 453

———. 2000a, A&AS, 141, 165

———. 2000b, in Disks, Planetesimals and Planets, ASP Conference Series, Vol. 219, 75–80

Masset, F. S., & Papaloizou, J. C. B. 2003, ApJ, 588, 494

Menou, K., & Goodman, J. 2004, ApJ, 606, 520

Nelson, R. P. 2005, A&A, 443, 1067

Nelson, R. P., & Papaloizou, J. C. B. 2004, MNRAS, 350, 849

Ogilvie, G. I., & Lubow, S. H. 2002, MNRAS, 330, 950

Pesenti, N., Dougados, C., Cabrit, S., Ferreira, J., Casse, F., Garcia, P., & O'Brien, D. 2004, A&A, 416, L9

Pollack, J. B., Hubickyj, O., Bodenheimer, P., Lissauer, J. J., Podolak, M., & Greenzweig, Y. 1996, Icarus, 124, 62

Tanaka, H., Takeuchi, T. & Ward, W. R. 2002, ApJ, 565, 1257

van Leer, B. 1977, Journal of Computational Physics, 23, 276

Ward, W. R. 1986, Icarus, 67, 164

———. 1997, Icarus, 126, 261

———. 1992, Abstracts of the Lunar and Planetary Science Conference, 23, 1491

———. 1991, Abstracts of the Lunar and Planetary Science Conference, 22, 1463